

Supporting Information for

# Novel hydrazone-based photoactivatable fluorescent probe with ultra-high photo-degradation efficiencies and their application in dynamic mitochondrial targeted bioimaging

*Jingming Zhou<sup>a, ‡</sup>, Xia Wang<sup>a, ‡</sup>, Xiaoxuan Ming<sup>a, ‡</sup>, Xuejing Su<sup>a</sup>, Yanbing Ke<sup>a</sup>, Wei Liu<sup>a</sup>, Tong Wu<sup>a</sup>, Yusheng Lu<sup>c, \*</sup>, Haipeng Xu<sup>b, \*</sup>, Lijun Xie<sup>a, d \*</sup>*

<sup>a</sup> Fujian Provincial Key Laboratory of Screening for Novel Microbial Products, Fujian Institute of Microbiology, Fuzhou, Fujian 350007, P.R. China

<sup>b</sup> Clinical Oncology School of Fujian Medical University, Fujian Cancer Hospital, Fuzhou, Fujian 350014, P.R. China

<sup>c</sup> Fujian-Taiwan-Hongkong-Macao Science and Technology Cooperation Base of Intelligent Pharmaceuticals, College of Material and Chemical Engineering, Minjiang University, Fuzhou, Fujian 350108, P.R. China

<sup>d</sup> Institute of Advanced Technology, University of Science and Technology of China, Hefei, Anhui 230088, P.R. China

‡ They are co-first authors

\* Corresponding author

Corresponding authors' e -mail: lu\_yu\_sheng@126.com (Y.L.),

penghaixu@163.com (H.X.),

Lijunxie8224@outlook.com (L.X.)

## Table of Contents

1. Experimental details.....	4
1.1 Reagents and materials .....	4
1.2 Apparatus .....	4
1.3 Methods .....	5
1.3.1 Thin layer chromatography (TLC) and column chromatography .....	5
1.3.2 NMR spectroscopy .....	5
1.3.3 LC-MS Analysis Methods .....	5
1.3.4 UV-Vis absorption and Emission spectroscopy .....	6
1.3.5 Irradiation experiments .....	6
1.3.6 The luminescence quantum yield determination .....	6
1.3.7 Molar absorption coefficient measurements .....	6
1.3.8 Photochemical quantum yield determination .....	7
1.3.9 Theoretical calculations .....	9
1.3.10 Cytotoxicity study and cell imaging.....	9
1.3.11 Detection of ROS in solution.....	9
1.3.12 Calculation of the release rate of Rh6G-CHO (R <sub>Rh6G-CHO</sub> ) .....	9
2. Supporting Figures.....	11
Figure S1. The HRMS spectrum of Rh6G-OH.....	11
Figure S2. The HRMS spectrum of Rh6G-CHO .....	11
Figure S3. The HRMS spectrum of LZ1 .....	11
Figure S4. The HRMS spectrum of LZ2 .....	11
Figure S5. The <sup>1</sup> H NMR of Rh6G-OH.....	12
Figure S6. The <sup>13</sup> C NMR of Rh6G-OH.....	12
Figure S7. The <sup>1</sup> H NMR of Rh6G-CHO .....	13
Figure S8. The <sup>13</sup> C NMR of Rh6G-CHO .....	13
Figure S9. The <sup>1</sup> H NMR of LZ1.....	14
Figure S10. The <sup>13</sup> C NMR of LZ1 .....	14
Figure S11. The <sup>1</sup> H NMR of LZ2.....	15
Figure S12. The <sup>13</sup> C NMR of LZ2.....	15

Figure S13. Absorbtion spectra of LZ1 (a) and absorbance at 530 nm (b) .....	16
Figure S14. Absorbtion spectra of LZ2 (a) and absorbance at 530 nm (b) .....	16
Figure S15. DAD 530 nm (a), MS data (b, c, d) of LZ2. ....	16
Figure S16. LC-MS chromatogram of LZ1 (10 $\mu$ M in EtOH) following irradiation at 530 nm for 1 minute, using a methanol/0.1% aq. HCOOH (68:32, v/v) mobile phase. ....	17
Figure S17. LC-MS chromatogram of LZ1 (10 $\mu$ M in EtOH) following irradiation at 530 nm for 1 minute, using a methanol/H <sub>2</sub> O (68:32, v/v) mobile phase. ....	17
Figure S18. Detection of ROS levels of blank sample (a), LZ1 (b) and LZ2 (c) under laser irradiation or in the dark. ....	17
Figure S19. Confocal images of mitochondrias stained with LZ2 (1 $\mu$ M) and Mito-Tracker Red (0.1 $\mu$ M) in live MCF-7 cells (under a 488 nm laser irradiation at different time intervals. Scale bar: 7.5 $\mu$ m) ..	18
Figure S20. Cytotoxicity of MCF-7 cells treated with different concentrations of LZ2 for 24 h as demonstrated by CCK-8 assay.....	18
Figure S21. The stability of LZ1 (a) and LZ2 (b) in pH = 7.4 and 8.0 solution with dark condition.....	19
Figure S22. The linear relationship between the concentration of Rh6G-CHO and the peak area of EIC at m/z399. ....	19
Figure S23. (a) Fluorescence microscopy images of MCF-7 cells stained with Rh6G-CHO (1 $\mu$ M), Mito-Tracker Red (0.1 $\mu$ M) and DAPI (0.1 $\mu$ M) (scale bar: 10 mm). (b) Correlation plot of the intensities of Rh6G-CHO and Mito-Tracker Red.....	19
3. Computational Details.....	20

## 1. Experimental details

### 1.1 Reagents and materials

All starting materials were obtained from commercial suppliers and used without further purification. Shanghai Macklin Biochemical Co. Ltd. (China) supplied rhodamin6G、phenyl hydrazine and 2-nitrobenzhydrazide. The reactions were monitored and purified using an HP-TLC Silica Gel 60 G254 plate (Cat. No. : C100006 and C100007) from Shanghai Haohong Scientific Co., Ltd. (China). Sinopharm Chemical Reagent Company (Beijing, China) provided all analytical grade reagents, including LiAlH<sub>4</sub>, pyridinium chlorochromate (PCC), DCM, THF, DMSO, and so forth. The breast cancer cell line MCF-7 were obtained from Procell Life Science & Technology Co., Ltd. and the Cell Bank of Type Culture Collection of the Chinese Academy of Sciences (Shanghai, China), respectively.

### 1.2 Apparatus

The Bruker AVANCE NEO 400MHz or 600 MHz spectrometer was used to record the purified chemicals found in the NMR analysis using the residual deuterated protons solvent DMSO-*D*<sub>6</sub>. And tetramethylcycline (TMS) were used as internal standards. An Agilent 6545 Q-TOF LC-MS was used to obtain high-resolution mass spectra (HRMS). On the Thermo Scientific Varioskan LUX 3020–80110, the absorbance and fluorescence spectra were finished. A Hitachi UH5300 UV-Vis spectrophotometer with a 1-cm quartz cuvette was used to record UV-Vis absorption spectra in the range of 800 ~ 200 nm and 298 K for calculating the molar absorption coefficient ( $\epsilon$ ). Irradiation experiments were done by the photoreaction instrument (WP-TEC-1020SL) that was purchased from WATTCAS (China). An Envision Plate Reader (PerkinElmer, USA) was used to collect data on cell viability. A CLSM (Leica, STELLARIS 5, Germany) was used to acquire fluorescent pictures of cells.

## 1.3 Methods

### 1.3.1 Thin layer chromatography (TLC) and column chromatography

Reactions were monitored on a thin-layer chromatography (TLC) Silica gel 60 G254 plate from Shanghai Haohong Scientific Co., Ltd. The purification of compounds was performed with silica gel (200-300 mesh) column chromatography.

### 1.3.2 NMR spectroscopy

$^1\text{H}$  and  $^{13}\text{C}$  NMR NMR spectra were acquired on a Bruker AVANCE NEO 400/600 MHz spectrometer in  $\text{DMSO}-\text{D}_6$  at ambient temperature with tetramethylsilane (TMS) as an internal standard. NMR standards used were as follows: ( $^1\text{H}$ -NMR)  $\text{DMSO}-\text{D}_6$  = 2.50 ppm. ( $^{13}\text{C}$ -NMR)  $\text{DMSO}-\text{D}_6$  = 39.52 ppm. All chemical shifts ( $\delta$ ) are reported in ppm relative to TMS. Spin multiplicities were reported as a singlet (s), doublet (d), triplet (t), quartet (q), multiplet (m) and broad (br) with coupling constant (J) reported in Hz.

### 1.3.3 LC-MS Analysis Methods

High-resolution mass spectra (HRMS) were obtained on an Agilent 6545 Q-TOF.

Analytical HPLC was performed on Agilent 1290 equipped with UV-Vis detector using reversed-phase (RP) C18 column (EclipsePlus, Length 50 mm, Internal dia. 2.1 mm, Particle size 1.8  $\mu\text{m}$ ) operating at 40°C, 530nm. The HPLC mobile phase comprised HPLC-grade acetonitrile and Millipore water, and Millipore water was containing 0.1% (v/v) formic acid. All the flow rates were set at 0.4 mL/min. The detailed information were listed in Tab. S1:

**Table S1 Gradient HPLC method**

Time (min)	0.1%HCOOH (%)	HPLC-grade acetonitrile (%)
0	60	40
5	60	40
8	0	100
10	0	100
10.01	60	40

To compare the UV-Vis absorption spectra of LZ1 and LZ1-isomer under consistent solvent conditions, an isocratic LC method was employed. Following irradiation at 530 nm for 1 min, LZ1 (10  $\mu$ M in EtOH) samples were analyzed separately with two mobile phases: methanol/0.1% aq. HCOOH (68:32, v/v) and methanol/H<sub>2</sub>O (68:32, v/v). Other chromatographic conditions were identical to those described previously.

#### **1.3.4 UV-Vis absorption and Emission spectroscopy**

UV-Vis absorption and Emission spectra, quantum yields and all the fluorescence measurements were recorded using a Varioskan LUX 3020-80110.

#### **1.3.5 Irradiation experiments**

Irradiation experiments were done in 1.0-cm quartz fluorescence cuvette. Light source was operated by the photoreaction instrument (WP-TEC-1020SL) that was purchased from WATTCAS (China).

#### **1.3.6 The luminescence quantum yield determination**

The luminescence quantum yield (QY) is measured using the following formula:

$$QY(\%) = Q_R \cdot \frac{I_s}{I_r} \cdot \frac{A_r}{A_s} \cdot \frac{N_s^2}{N_r^2} \cdot 100$$

$Q_R$  is the quantum yield of Rhodamine 6G in Ethanol;  $A_s$  and  $A_r$  are the optical density (absorbance) of sample and Rhodamine 6G, respectively;  $I_s$  and  $I_r$  are the integrated intensities (areas) of sample and standard spectra, respectively; the refractive indices of the sample and reference solution are  $N_s$  and  $N_r$ , respectively; The subscripts r and s stand for sample and Rhodamine 6G, respectively.

#### **1.3.7 Molar absorption coefficient measurements**

To prepare stock solutions of compounds Rh6G-CHO, LZ1, and LZ2, approximately 1.0 mg of each sample was accurately weighed using an analytical balance (Mettler Toledo XSE105DU) and dissolved in 1.0 mL of EtOH in a 5-mL centrifuge tube. Serial dilutions were subsequently prepared from these stock solutions. Appropriate concentrations were selected, and the UV-Vis absorption spectra of the solutions were recorded

over the range of 200-800 nm at 298 K using a Hitachi UH5300 UV-Vis spectrophotometer with a 1-cm standard quartz cuvette. Baseline correction was applied prior to data analysis. The molar absorption coefficients at various wavelengths were calculated from the absorbance measurements using the Beer-Lambert law:

$$\varepsilon = \frac{A}{c \cdot l}$$

where  $\varepsilon$  is the molar absorption coefficient ( $\text{L} \cdot \text{mol}^{-1} \cdot \text{cm}^{-1}$ ), A is the absorbance, c is the concentration ( $\text{mol/L}$ ) and l is the path length (cm).

### 1.3.8 Photochemical quantum yield determination

1) The quantum yield for the photoreaction of the degradation of the **LZ1/LZ2** was assessed in the following manner.

$$\Phi_d = \frac{\Delta M}{N_p} \quad \text{eq.0}_d$$

$\Delta M$  Number of **LZ1/LZ2** molecules degraded

$N_p$  Number of absorbed photons

The calculation of the number of **LZ1/LZ2** molecules degraded was carried out using equation **1<sub>d</sub>**.

$$\Delta M = \Delta c \cdot V \cdot N_a \quad \text{eq.1}_d$$

$V$  Irradiated volume

$N_a$  Avogadro's number 530

$\Delta c$  Concentration decreases of the **LZ1/LZ2**

2) The quantum yield for the photoreaction of aldehyde hydrazone cage to **Rh6G-CHO** was assessed in the following manner.

$$\Phi_u = \frac{\Delta M}{N_p} \quad \text{eq.0}_u$$

$\Delta M$  Number of **Rh6G-CHO** molecules generated

$N_p$  Number of absorbed photons

The calculation of the number of **Rh6G-CHO** molecules generated was carried out using equation **1<sub>u</sub>**.

$$\Delta M = \Delta c \cdot V \cdot N_a \quad \text{eq.1}_u$$

$V$  Irradiated volume

$N_a$  Avogadro's number 530

$\Delta c$  Concentration increases of the **Rh6G-CHO**

The number of absorbed photons ( $N_p$ ) can be evaluated from the measured the optical power absorbed by the test solution ( $P_a$ ), irradiated time ( $\Delta T$ ) and the energy of a photon of 530 nm wavelength ( $E_p$ ) according to equation 2.

$$N_p = \frac{P_a \cdot \Delta T}{E_p} \quad \text{eq.2}$$

$P_a$  can be found by the following equation 3.

$$P_a = E_e \cdot S \cdot (1 - 10^{-A}) \quad \text{eq.3}$$

when imported Lambert-Beer law ( $A = \varepsilon \cdot C \cdot L$ ), the equation becomes.

$$P_a = E_e \cdot S \cdot (1 - 10^{-\varepsilon \cdot C \cdot L}) \quad \text{eq.4}$$

$A$  Corresponding absorbance of test solution at the irradiation wavelength

$E_e$  Intensity of incident light at the irradiation wavelength

$S$  Cross-sectional area of irradiation

$\varepsilon$  Molar absorption coefficient

$C$  Concentration of the **LZ1/LZ2**

$L$  Optical path length

The energy of a photon  $E_p$  is calculated by equation 5.

$$E_p = \frac{h \cdot c}{\lambda} \quad \text{eq.5}$$

$h$  Planck's constant

$c$  Speed of light

$\lambda$  Irradiation wavelength

**The procedure for the measurement followed steps below.**

5.0 mL EtOH solution of staurosporine aldehyde-hydrazone cage (10  $\mu\text{M}$ ) in a flat-bottomed quartz tube was exposed to light irradiation at 530 nm under ambient condition. The inner diameter of the flat-bottomed tubes was measured by micrometer and calculated by the formula for circular area ( $2.270 \text{ cm}^2$ ). The light source operated with a current stabilizer. The incident light intensity ( $180.5 \text{ mW} \cdot \text{cm}^{-2}$ ) was measured with a power-meter (WATTCAS WP-TEC-1020SL, China).

A 0.5- $\mu$ L portion of this solution was then subjected to LC-MS analysis following the photodegradation. The area of peaks from the EIC trace were integrated and the concentrations of the product were quantified by pure **Rh6G-CHO** as reference (0.1, 1, 10  $\mu$ M).

### 1.3.9 Theoretical calculations

Density functional theory (DFT) calculations were carried out using the B3LYP functional and the 6-31G basis set. For the HOMO-LUMO computations, the DFT model was employed using the above functional and the def2-TZVP basis set.

### 1.3.10 Cytotoxicity study and cell imaging

**Cytotoxicity study** MCF-7 (breast cancer cells) were containing in 10% (v/v) fetal bovine serum (FBS, Gibco) and 1% antibiotics (100 units/mL penicillin and 100 mg/mL streptomycin) in 5% CO<sub>2</sub> humidity incubator at 37°C. The cells containing the different concentration of **LZ1** or **LZ2** was incubated for 24 h, respectively. 10  $\mu$ L of CCK-8 reagent were added to each well after the initial 24 h of incubation, and the plate was then incubated for an additional 3 h at 37 °C in the dark. Using a microplate reader, the absorbance at 450 nm in each well was calculated. Three parallel tests were set up with all of the samples.

**Mitochondrion Colocalization experiment:** MCF-7 cells were cultured on a confocal dish for 24 h. Subsequently, the culture medium was replaced with a medium containing 1 $\mu$ M **LZ1** (or **LZ2**) and 0.1 $\mu$ M Mito-Tracker Red CMXRos (Beyotime, China). After incubation for 30 min, these cells were washed with PBS and resuspended in fresh medium. Images were immediately acquired using a confocal microscope (Leica, STELLARIS 5, Germany), employing consistent acquisition parameters across all experimental groups (63x optical magnification and 4x digital magnification).

### 1.3.11 Detection of ROS in solution

The production of ROS under laser irradiation was detected by DCFH-DA. The 96-well plate was added with 100  $\mu$ L of PBS solution containing DCFH-DA (10  $\mu$ M) and **LZ1** (or **LZ2**) (0, 10  $\mu$ M, respectively). Then the PBS solution was exposed to dark or 530 nm laser irradiation (150 mW·cm<sup>-2</sup>) for different durations ranging from 0 to 40 minutes. The fluorescence intensity of DCFH-DA (ROS levels) in PBS was detected using a multifunctional microplate reader (TECAN, M200 PRO, Switzerland) with excitation at 488 nm and emission at 529 nm.

### 1.3.12 Calculation of the release rate of Rh6G-CHO ( $R_{Rh6G-CHO}$ )

Prepare 0.1, 0.5, 1, 3, 5, 8, and 10  $\mu$ M Rh6G-CHO control solutions. After liquid chromatography-mass spectrometry analysis, fit a linear curve using the EIC Area at m/z 399 and the concentration of Rh6G-CHO. After exposing 10  $\mu$ M of LZ1 or LZ2 solution to 530 nm light for a certain period of time, the EIC Area of Rh6G-CHO at m/z 399 was determined by liquid chromatography-mass spectrometry. The peak area was then used to calculate the concentration of Rh6G-CHO ( $C_{Rh6G-CHO}$ ,  $\mu$ M) based on the standard curve (Figure S22).

$$R_{Rh6G-CHO} = C_{Rh6G-CHO} / 10 \times 100\%$$

## 2. Supporting Figures.

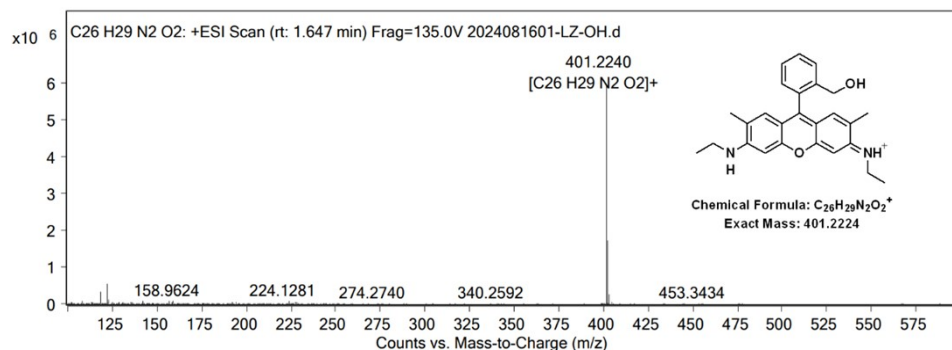


**Figure S1. The HRMS spectrum of Rh6G-OH.**

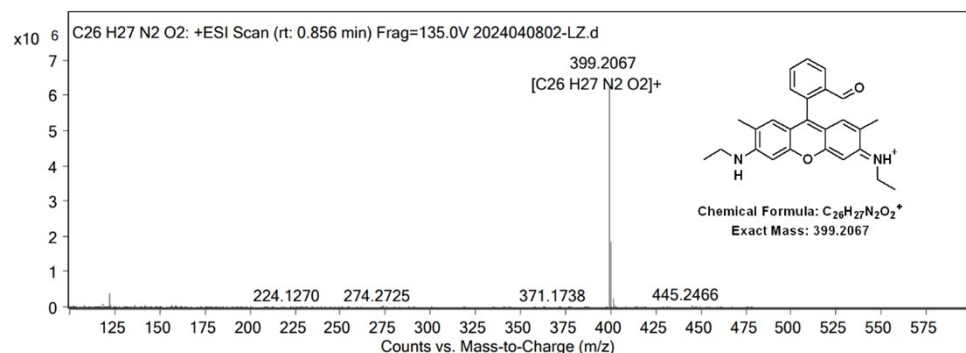


**Figure S2. The HRMS spectrum of Rh6G-CHO.**

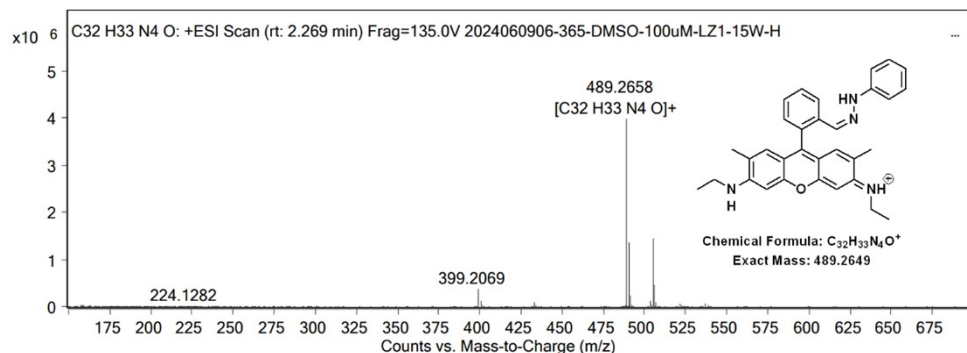


**Figure S3. The HRMS spectrum of LZ1.**

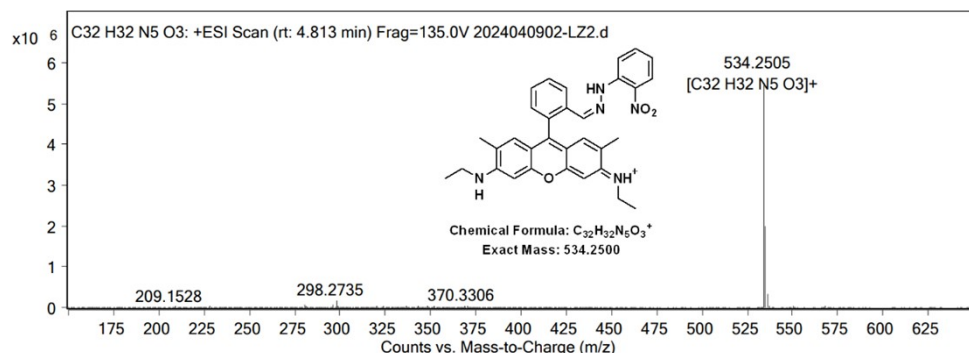


**Figure S4. The HRMS spectrum of LZ2.**

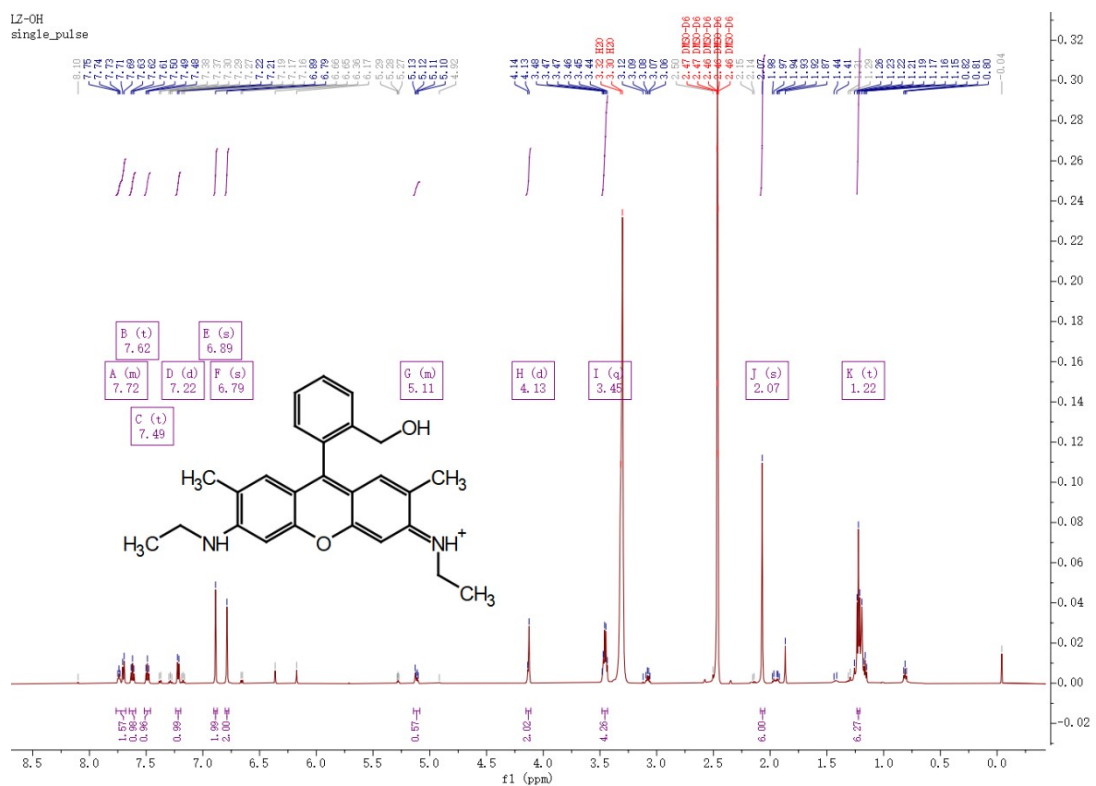


**Figure S5.** The  $^1\text{H}$  NMR of Rh6G-OH.

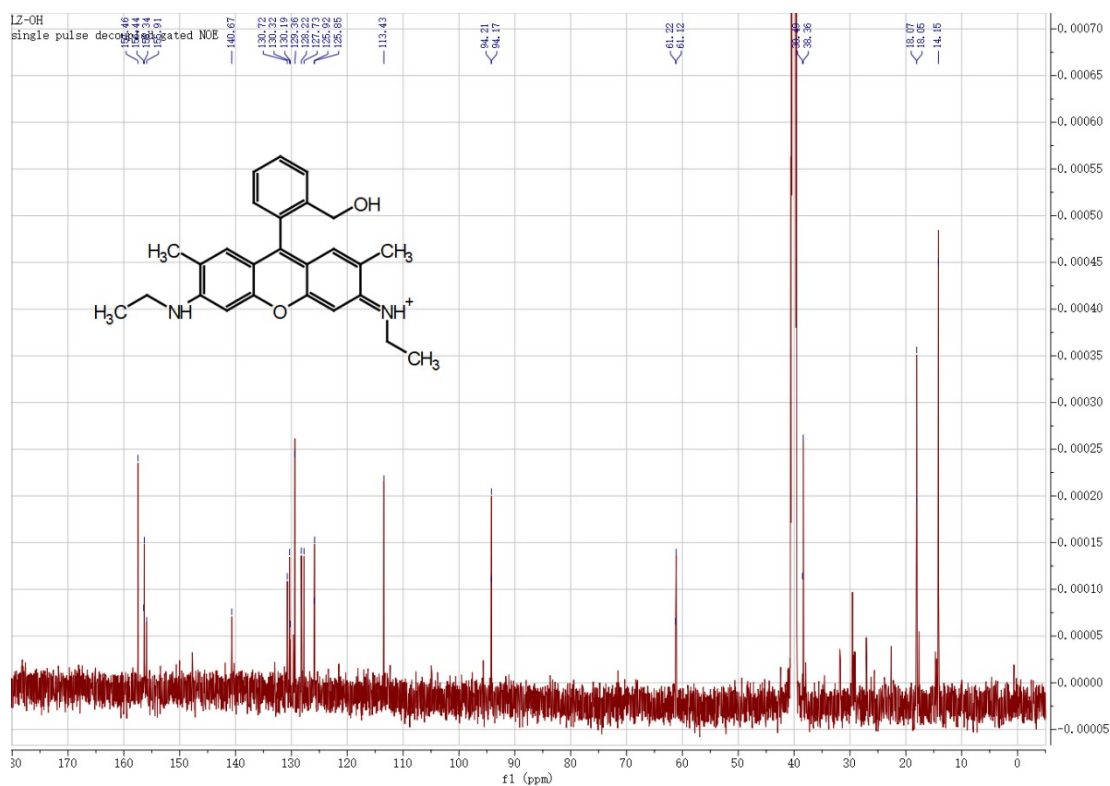


**Figure S6.** The  $^{13}\text{C}$  NMR of Rh6G-OH.

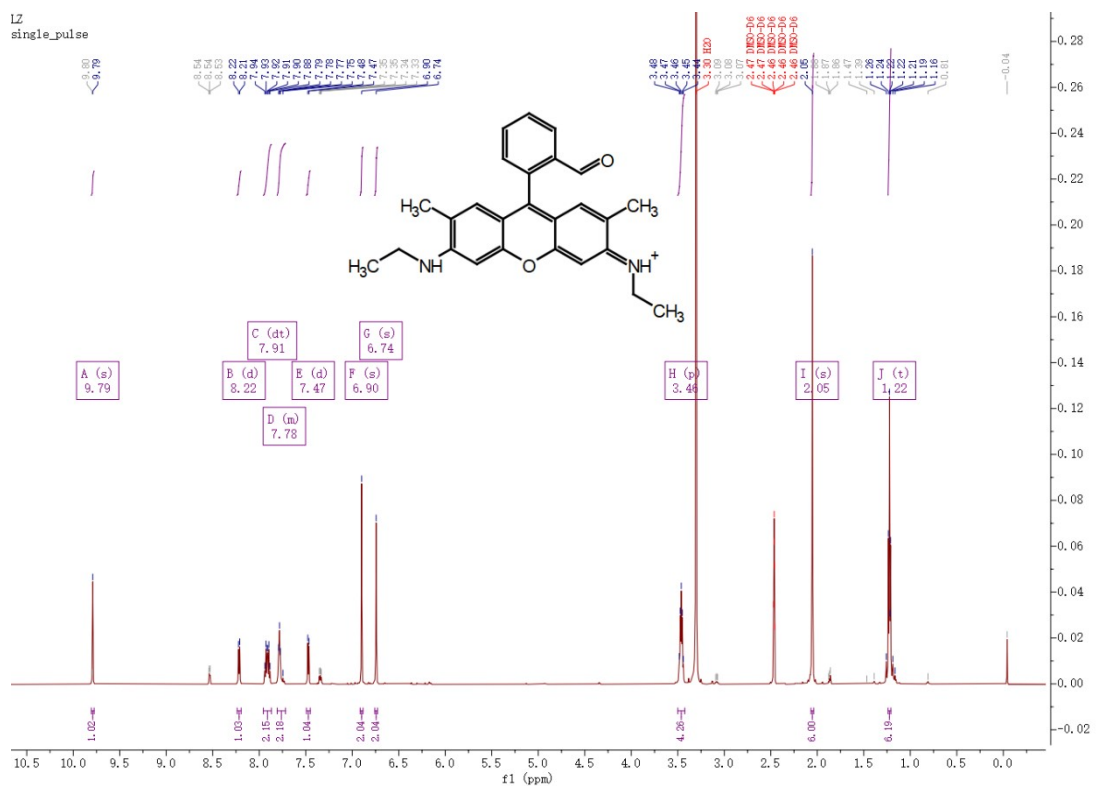


Figure S7. The  $^1\text{H}$  NMR of Rh6G-CHO.

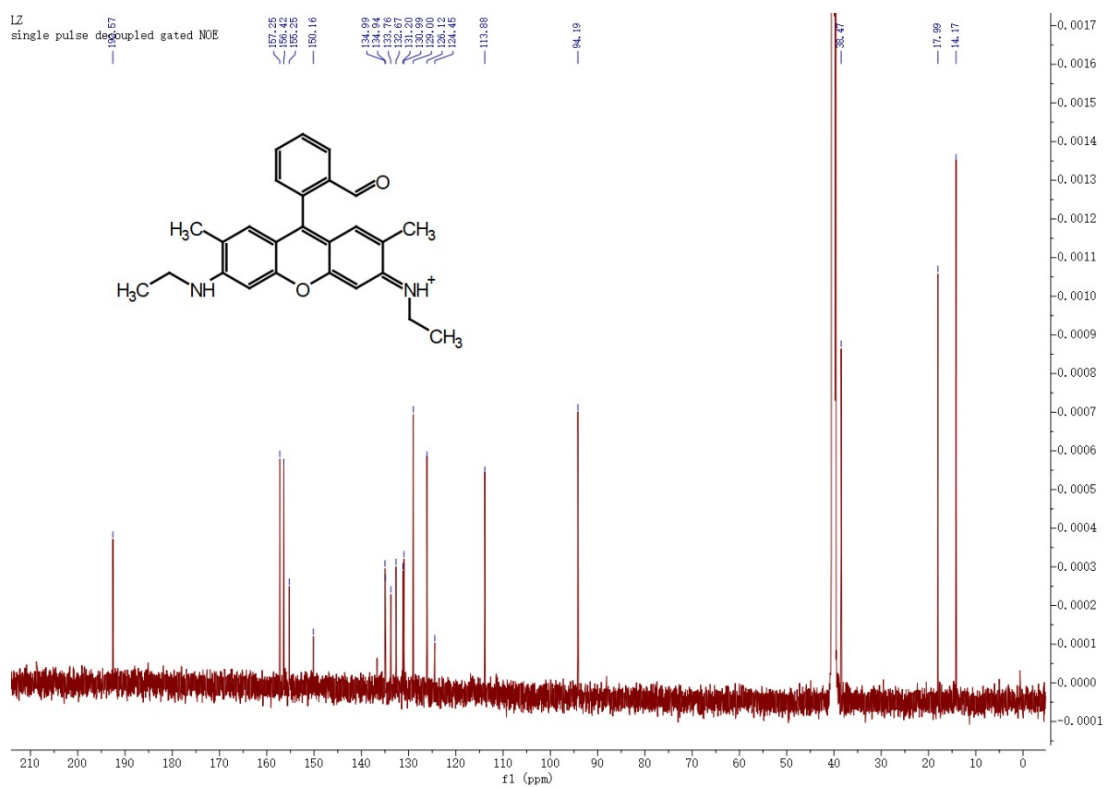


Figure S8. The  $^{13}\text{C}$  NMR of Rh6G-CHO.

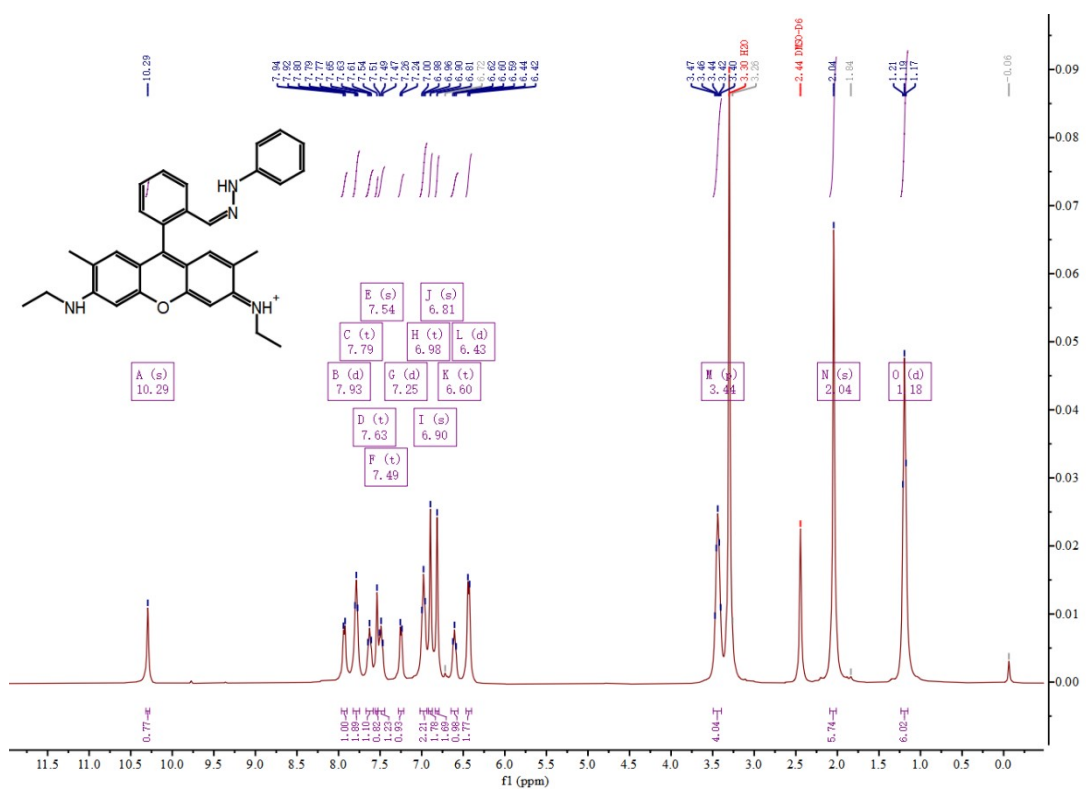


Figure S9. The  $^1\text{H}$  NMR of LZ1.

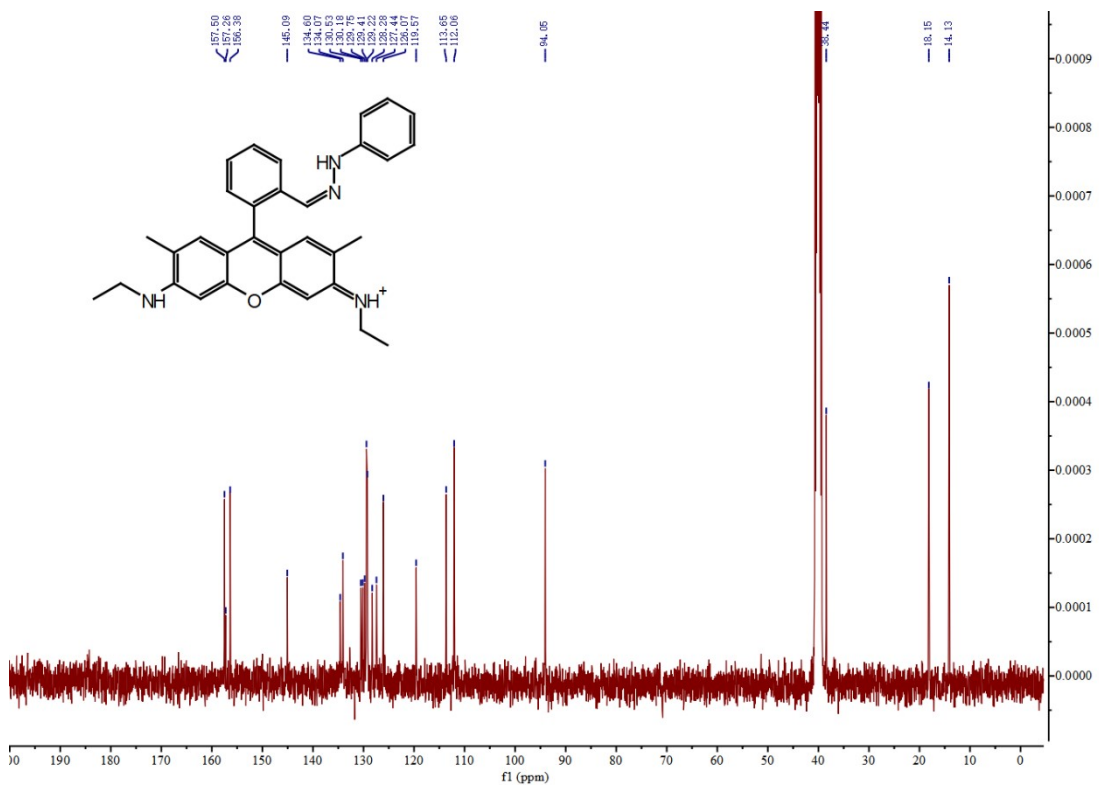


Figure S10. The  $^{13}\text{C}$  NMR of LZ1.

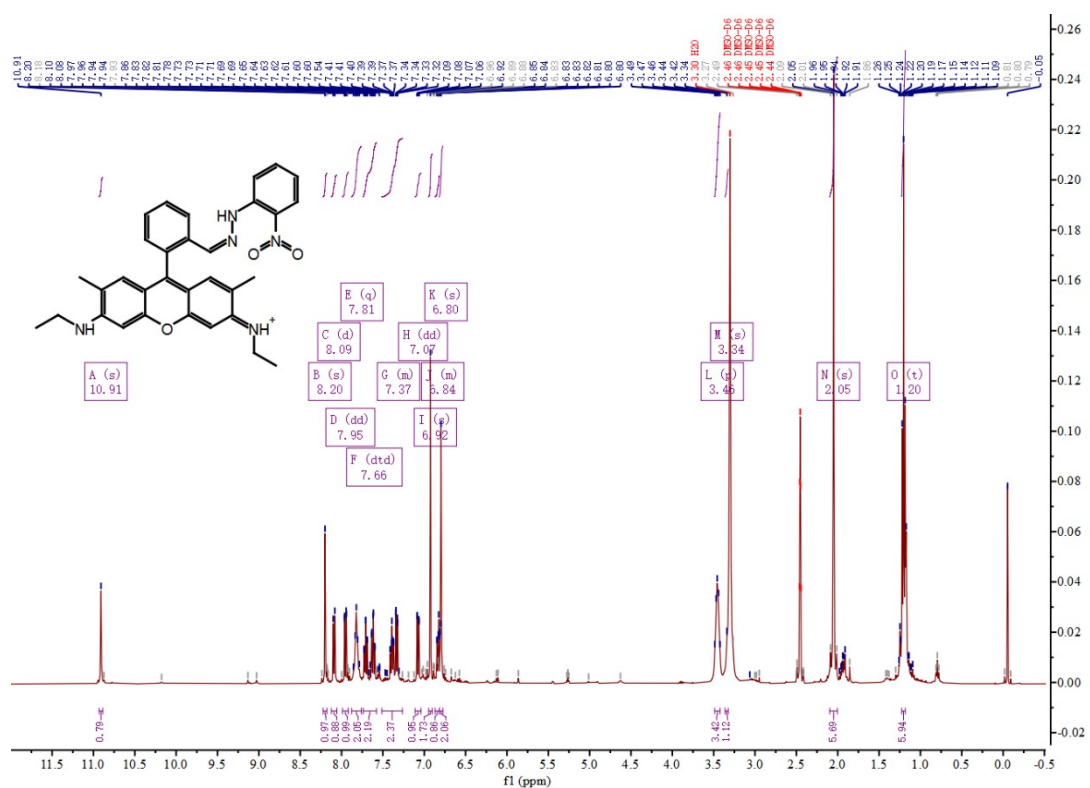


Figure S11. The  $^1\text{H}$  NMR of LZ2.

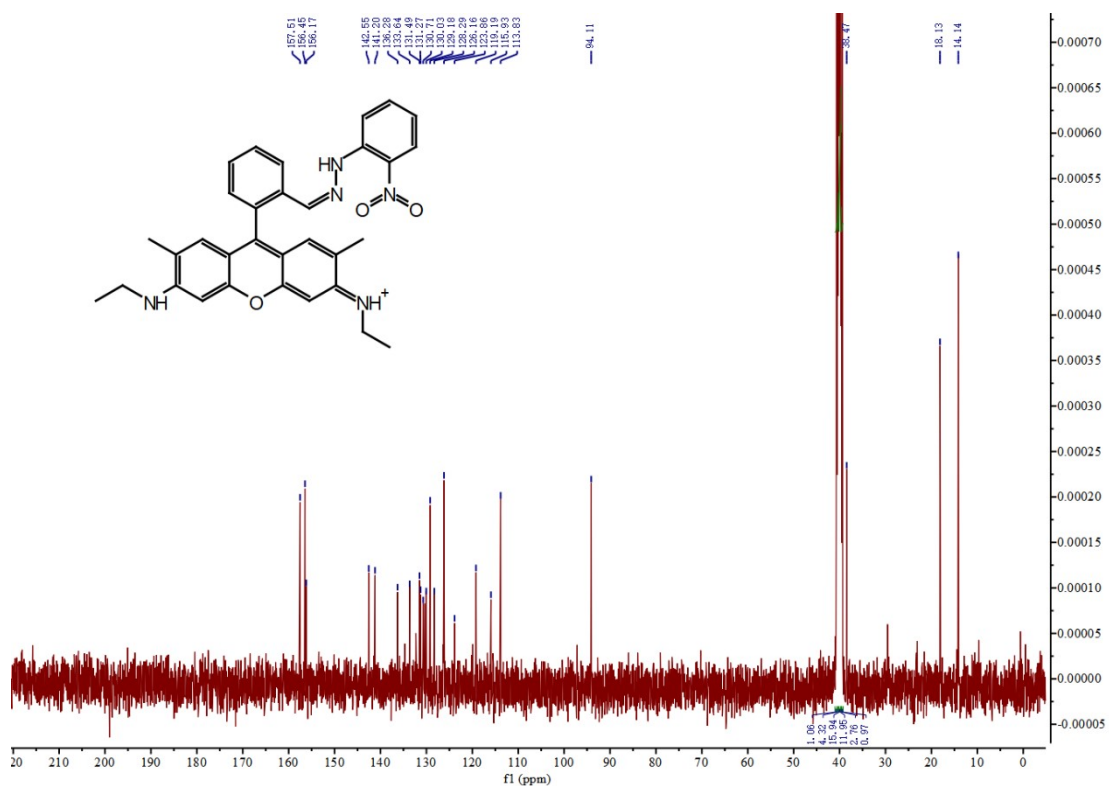
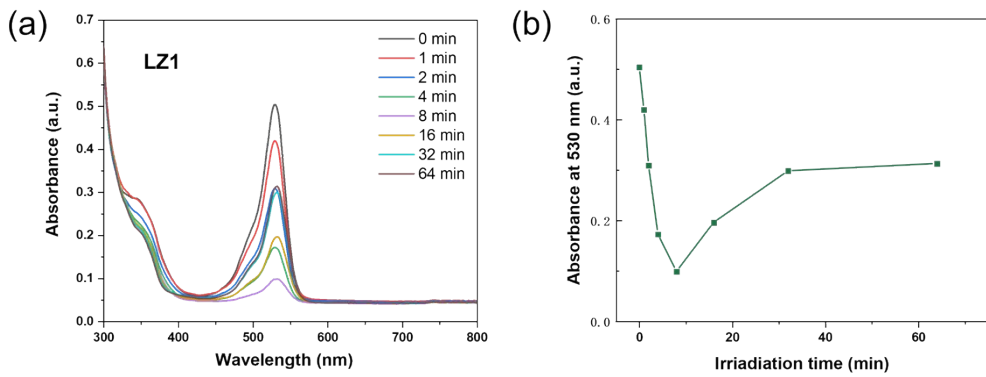
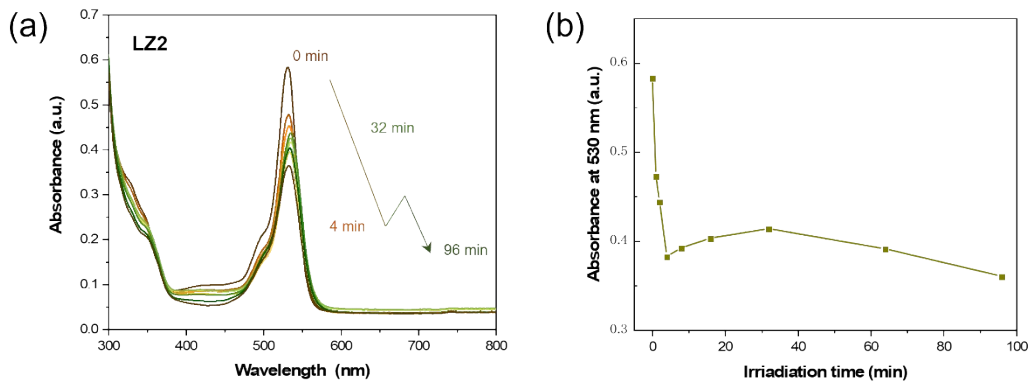


Figure S12. The  $^{13}\text{C}$  NMR of LZ2.



**Figure S13. Absorbtion spectra of LZ1 (a) and absorbance at 530 nm (b)**



**Figure S14. Absorbtion spectra of LZ2 (a) and absorbance at 530 nm (b)**

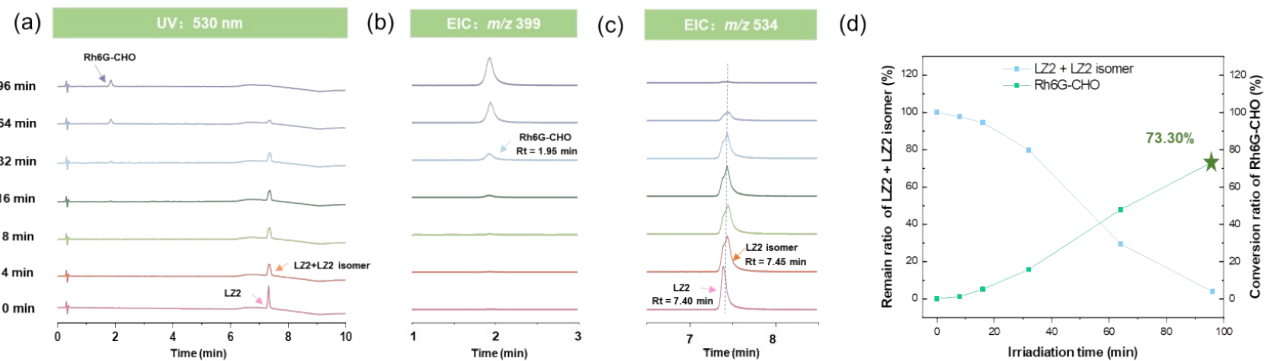


**Figure S15. DAD 530 nm (a), MS data (b, c, d) of LZ2.**

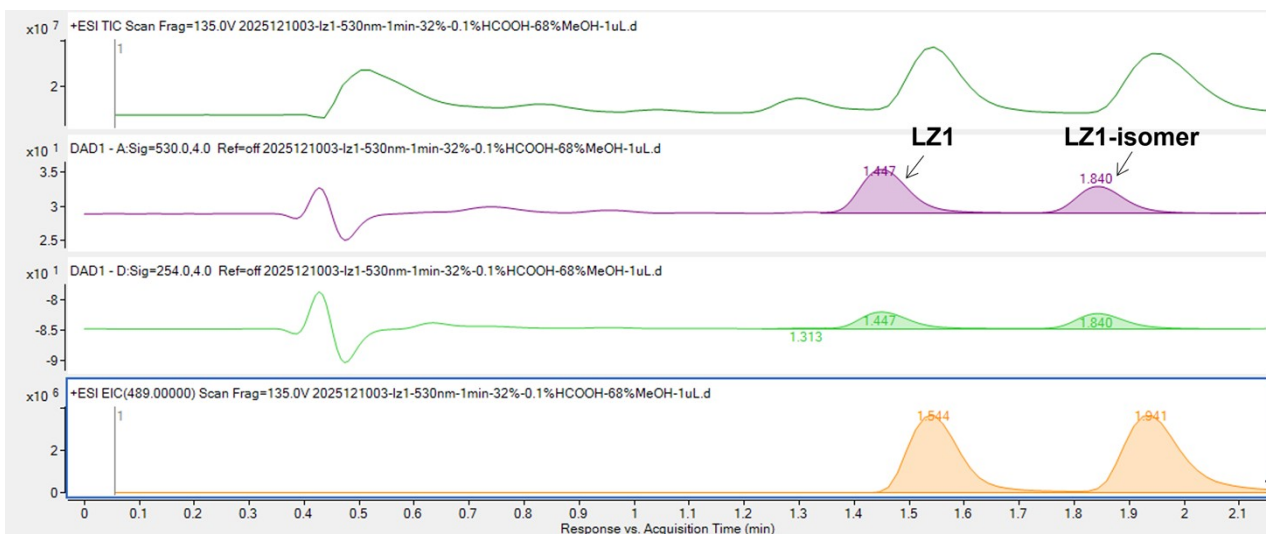


**Figure S16.** LC-MS chromatogram of LZ1 (10  $\mu$ M in EtOH) following irradiation at 530 nm for 1 minute, using a methanol/0.1% aq. HCOOH (68:32, v/v) mobile phase.

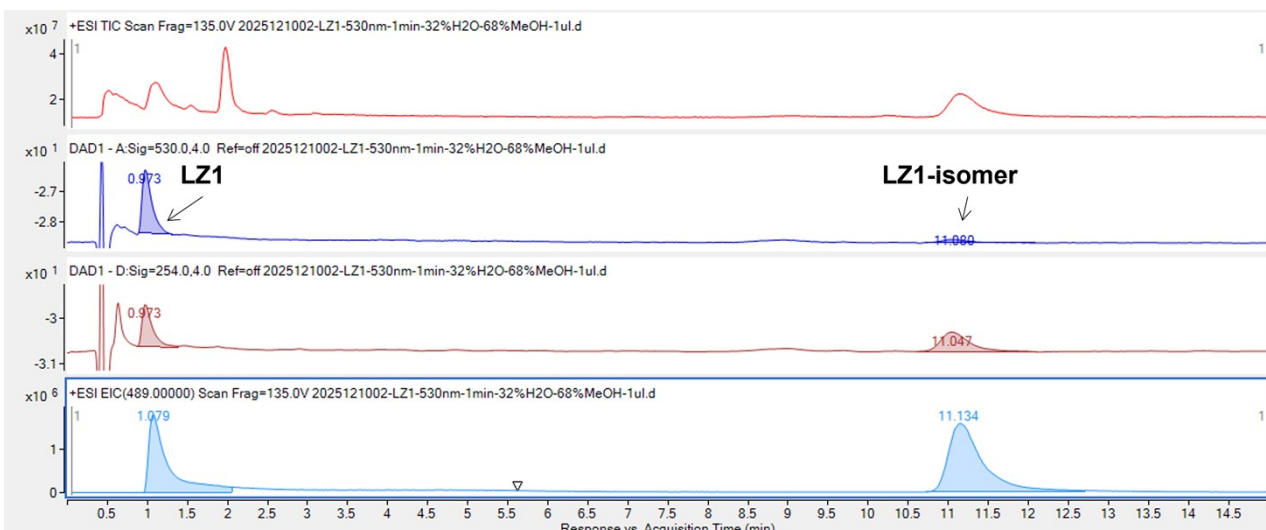


**Figure S17.** LC-MS chromatogram of LZ1 (10  $\mu$ M in EtOH) following irradiation at 530 nm for 1 minute, using a methanol/H<sub>2</sub>O (68:32, v/v) mobile phase.

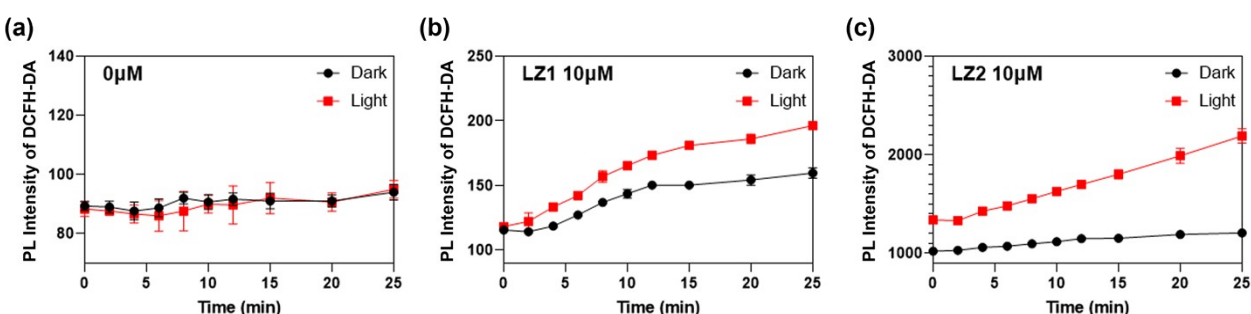


**Figure S18.** Detection of ROS levels of blank sample (a), LZ1 (b) and LZ2 (c) under laser irradiation or in the dark.

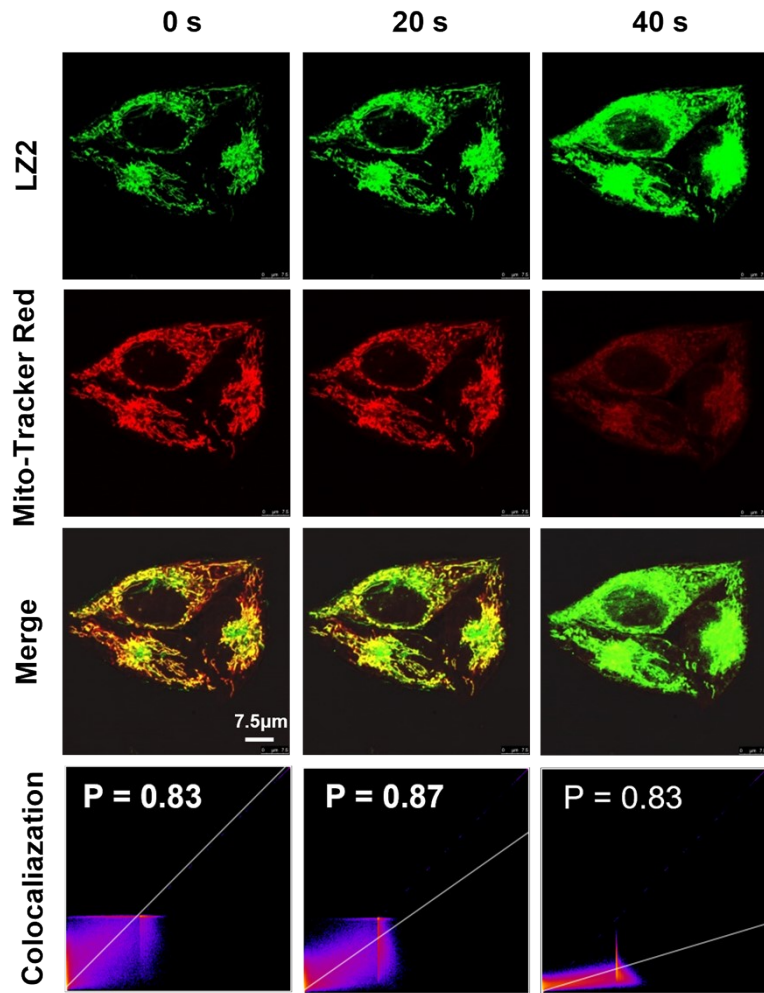


**Figure S19.** Confocal images of mitochondria stained with LZ2 (1  $\mu$ M) and Mito-Tracker Red (0.1  $\mu$ M) in live MCF-7 cells (under a 488 nm laser irradiation at different time intervals. Scale bar: 7.5  $\mu$ m) .

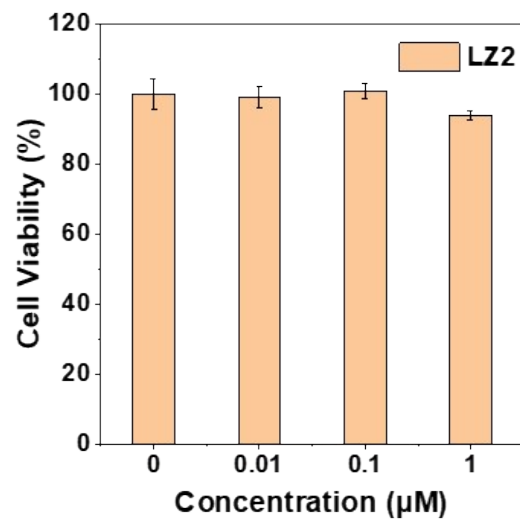


**Figure S20.** Cytotoxicity of MCF-7 cells treated with different concentrations of LZ2 for 24 h as demonstrated by CCK-8 assay.

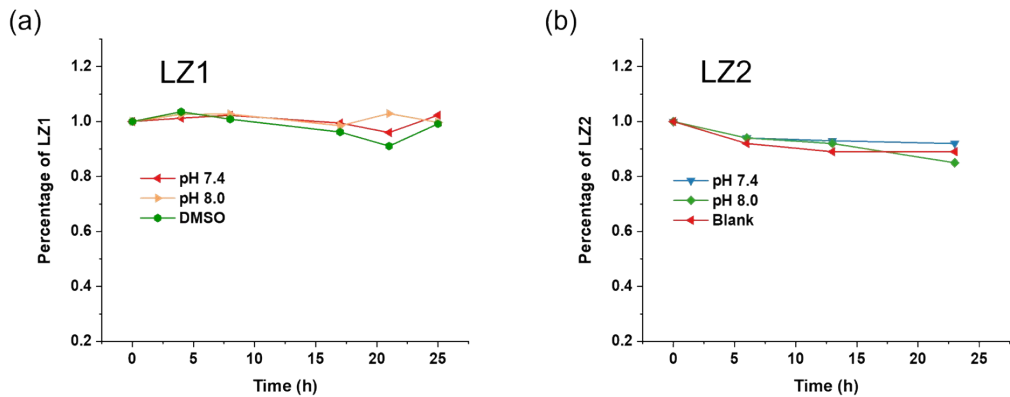


**Figure S21.** The stability of LZ1 (a) and LZ2 (b) in pH = 7.4 and 8.0 solution with dark condition.

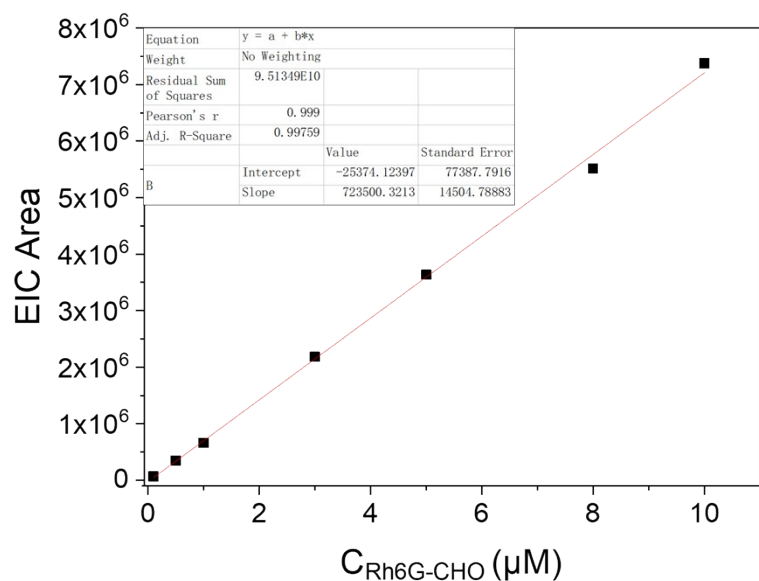


**Figure S22.** The linear relationship between the concentration of Rh6G-CHO and the peak area of EIC at m/z399.

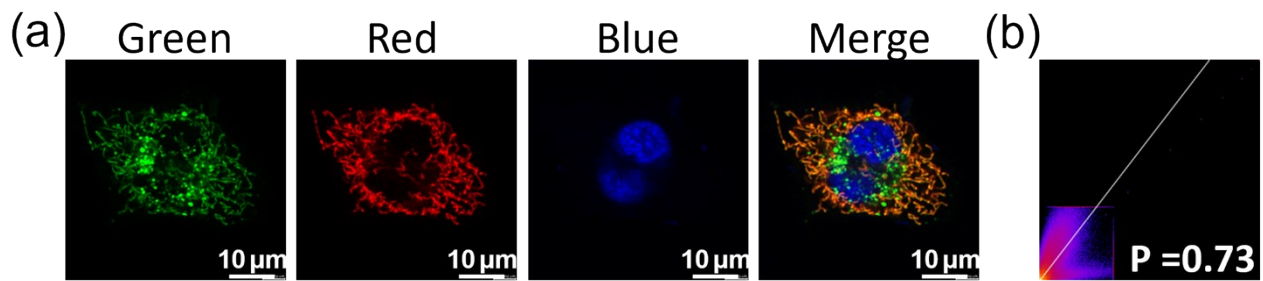


**Figure S23.** (a) Fluorescence microscopy images of MCF-7 cells stained with Rh6G-CHO (1  $\mu\text{M}$ ), Mito-Tracker Red (0.1  $\mu\text{M}$ ) and DAPI (0.1  $\mu\text{M}$ ) (scale bar: 10 mm). (b) Correlation plot of the intensities of Rh6G-CHO and Mito-Tracker Red.

### 3. Computational Details

#### LZ1

C	0.22267400	2.98360600	-0.44829400
C	-0.86875700	2.24965700	-1.02731600
C	-1.03497400	0.81282700	-0.76738900
C	-2.25444500	0.30542300	-0.19041900
C	-0.03546700	-0.10415400	-1.07815800
C	-2.37640300	-1.07198600	0.04910000
C	-0.19000900	-1.48657400	-0.74388600
C	-4.50617000	0.58794300	0.73501300
O	-1.36605100	-1.93323800	-0.21067000
C	2.17761400	-0.65414300	-1.98760200
C	-4.61054900	-0.81725000	0.92370500
C	2.06994200	-2.03069300	-1.48819800
C	4.34073500	-4.87927900	-1.35761900
H	5.14307900	-4.38692000	-0.80022400
H	4.28252800	-5.92217000	-1.03038400
H	4.61583000	-4.86108700	-2.41548300
C	3.02175900	-4.15596000	-1.14585600
H	2.22375700	-4.69855200	-1.68107800
H	2.74481800	-4.20099800	-0.07790400
C	-6.45099400	-3.38921900	0.25218900
H	-5.66111800	-3.28510500	-0.49562500
H	-6.65144500	-4.45573600	0.39087300
H	-7.35638000	-2.92367100	-0.14786300
C	-6.04912800	-2.74240900	1.57384800
H	-6.85415600	-2.85707100	2.30582600
H	-5.18221400	-3.25617700	2.00193500

C	3.40655400	-0.28062300	-2.75215800
H	4.30968100	-0.43879600	-2.15516200
H	3.52095800	-0.92828800	-3.62645000
H	3.36620600	0.76112400	-3.07849500
C	-5.63800900	1.48587900	1.13743300
H	-6.55054800	1.28360100	0.56038900
H	-5.88937100	1.37043600	2.19895200
H	-5.37823400	2.53212400	0.96981400
C	-3.34604700	1.10365000	0.19938000
H	-3.26093100	2.17768400	0.07233100
C	-3.52690700	-1.62995600	0.58142000
H	-3.54687200	-2.70276700	0.72360200
C	0.79669200	-2.40662500	-0.92485800
H	0.60511100	-3.42926000	-0.62590400
C	1.17925500	0.23420400	-1.76563100
H	1.27606500	1.25065300	-2.13296500
C	0.48836100	4.29047200	-0.94635900
H	1.35044400	4.82127500	-0.55802400
C	-0.34705200	4.88043200	-1.86175100
H	-0.13294100	5.88455300	-2.21484200
C	-1.47976100	4.19978300	-2.34227500
H	-2.13399200	4.66656400	-3.06976500
C	-1.71929900	2.89808100	-1.92238400
H	-2.54359800	2.33726500	-2.35346400
N	-5.75019400	-1.33092000	1.48839600
H	-6.54311500	-0.71226300	1.50621100
N	3.11633100	-2.79297000	-1.60601400
C	0.97441300	2.42890500	0.60257400
H	0.59510700	1.52501300	1.08054600
N	2.14850600	2.92131300	1.01164400

N	2.68168200	2.38458000	2.11836400
H	2.53040500	2.88317300	2.99383100
C	3.54562900	1.34604100	2.16228800
C	3.78157400	0.55181800	1.01784500
C	4.17559300	1.03238900	3.39072300
C	4.59503700	-0.55430300	1.12365500
H	3.29153100	0.80655000	0.08828100
C	5.00137000	-0.06502500	3.46700600
H	3.99478200	1.65615800	4.26056300
C	5.21040200	-0.86643100	2.33970500
H	4.73085200	-1.19485300	0.25883900
H	5.48570400	-0.31131700	4.40484800
H	5.85040000	-1.73811900	2.41102500

## LZ2

C	-0.23296100	2.99119000	-0.62453400
C	0.73419100	2.23915000	-1.31796500
C	0.96434200	0.80012100	-1.04089100
C	-0.03569100	-0.14411800	-1.29781400
C	2.21057100	0.34791100	-0.55382000
C	0.21484900	-1.52325800	-1.03445000
C	2.41745200	-1.04682500	-0.37100900
C	-2.31622900	-0.72751300	-1.94862700
O	1.42605100	-1.93407800	-0.61836400
C	4.49132200	0.75764000	0.22793100
C	-2.05535700	-2.09687700	-1.54156500
C	4.70371100	-0.68099800	0.37062600
C	7.59641300	-2.68095400	1.39059900
H	7.78412100	-2.17010400	2.33779000

H	7.81067800	-3.74484000	1.52210400
H	8.28926300	-2.27748200	0.64843700
C	6.16114600	-2.46722700	0.94787600
H	5.97288200	-3.01281900	0.00887000
H	5.47182000	-2.90366400	1.68892400
C	-2.52527600	-5.30895200	-2.07906800
H	-1.51944000	-5.06676000	-2.43184800
H	-2.50193800	-6.31580800	-1.65416600
H	-3.19068300	-5.31707900	-2.94555900
C	-3.01156900	-4.31246200	-1.03686000
H	-4.01981200	-4.57162800	-0.71056800
H	-2.38256200	-4.33736500	-0.14000100
C	5.60466300	1.68465800	0.58060900
H	5.90089300	1.54988300	1.62432900
H	6.49368400	1.46352400	-0.01592800
H	5.31243100	2.72370100	0.42199500
C	-3.66401500	-0.34941300	-2.47076100
H	-3.99266900	-1.03972300	-3.25484000
H	-4.38893200	-0.34297900	-1.65020000
H	-3.63764700	0.65872400	-2.88418100
C	-1.32213000	0.18724700	-1.81227400
H	-1.51223300	1.21920900	-2.07900900
C	-0.75288800	-2.48322300	-1.17608000
H	-0.51138200	-3.50524600	-0.91975600
C	3.60854900	-1.55529900	0.06480100
H	3.70157700	-2.62711300	0.18094900
C	3.28759800	1.21625200	-0.21577700
H	3.12251300	2.28218800	-0.31835700
C	-0.43771300	4.31785500	-1.02494900
H	-1.18495600	4.89071500	-0.48860200

C	0.27960000	4.88036200	-2.06600000
H	0.09381200	5.91090900	-2.35075800
C	1.24410600	4.13470000	-2.73726200
H	1.81410800	4.56961700	-3.55083700
C	1.46803800	2.82166800	-2.35685200
H	2.20163800	2.22127300	-2.88617000
N	-3.07751600	-2.95296500	-1.54377200
H	-3.97631600	-2.49723400	-1.44967700
N	5.88304800	-1.06603600	0.77992900
C	-1.02187700	2.43456700	0.48447000
H	-0.61176400	1.61394700	1.07610300
N	-2.18068900	2.93461100	0.69905200
N	-2.95270100	2.54951700	1.72766200
H	-3.91827300	2.59551500	1.42852700
C	-2.66979000	1.35911400	2.47320600
C	-1.89323400	1.49879800	3.61306600
C	-3.12869100	0.07177200	2.09663100
C	-1.51991400	0.40530100	4.38935100
H	-1.57765100	2.50298900	3.87719100
C	-2.74095600	-1.02877900	2.88214000
C	-1.95223300	-0.86178300	4.00459100
H	-0.91087300	0.54263000	5.27486100
H	-3.09840000	-2.00134100	2.57273900
H	-1.68085800	-1.73142200	4.59489400
N	-3.96151200	-0.15457900	0.99738100
O	-4.50307800	0.82366600	0.38993600
O	-4.11842500	-1.35706500	0.59529800